

# A Reductant-Resistant and Metal-Free Fluorescent Probe for Nitroxyl Applicable to Living Cells

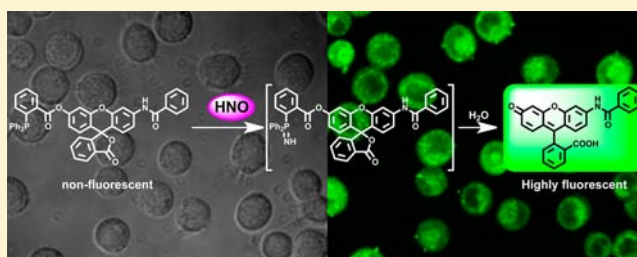
Kodai Kawai,<sup>†</sup> Naoya Ieda,<sup>†</sup> Kazuyuki Aizawa,<sup>†</sup> Takayoshi Suzuki,<sup>†,¶</sup> Naoki Miyata,<sup>†</sup> and Hidehiko Nakagawa<sup>\*,†,§</sup>

<sup>†</sup>Graduate School of Pharmaceutical Sciences, Nagoya City University, 3-1 Tanabe-dori, Mizuho-ku, Nagoya, Aichi 467-8603, Japan

<sup>§</sup>Japan Science and Technology Agency, PRESTO, 4-1-8 Honcho Kawaguchi, Saitama 332-0012, Japan

## Supporting Information

**ABSTRACT:** Nitroxyl (HNO) is a one-electron reduced and protonated derivative of nitric oxide (NO) and has characteristic biological and pharmacological effects distinct from those of NO. However, studies of its biosynthesis and activities are restricted by the lack of versatile HNO detection methods applicable to living cells. Here, we report the first metal-free and reductant-resistant HNO imaging probe available for use in living cells, P-Rhod. It consists of a rhodol derivative moiety as the fluorophore, linked via an ester moiety to a diphenylphosphinobenzoyl group, which forms an aza-ylide upon reaction with HNO. Intramolecular attack of the aza-ylide on the ester carbonyl group releases a fluorescent rhodol derivative. P-Rhod showed high selectivity for HNO in the presence of various biologically relevant reductants, such as glutathione and ascorbate, in comparison with previous HNO probes. We show that P-Rhod can detect not only HNO enzymatically generated in the horseradish peroxidase-hydroxylamine system *in vitro* but also intracellular HNO release from Angeli's salt in living cells. These results suggest that P-Rhod is suitable for detection of HNO in living cells.



## INTRODUCTION

Since the biosynthesis of nitric oxide (NO) in mammalian systems was discovered in the late 1980s, there has been increasing interest in the biological roles of reactive nitrogen species (RNS).<sup>1</sup> NO mediates both physiological and pathological processes, including cardiovascular signaling in the circulatory system, neurotransmission in the central nervous system, and rejection of foreign substances by the immune system.<sup>2</sup> As for other RNS, peroxyxynitrite (ONOO<sup>-</sup>) is thought to be involved in various diseases and regulation of nitration of biomolecules,<sup>3</sup> and dinitrogen trioxide (N<sub>2</sub>O<sub>3</sub>), nitrite (NO<sub>2</sub><sup>-</sup>), and nitrogen dioxide (NO<sub>2</sub>) are involved in alkylation of DNA.<sup>4</sup> Also, there is increasing evidence that nitroxyl (HNO), the one-electron reduced form of NO, has biological effects distinct from those of NO.<sup>5</sup> For example, HNO reacts directly with protein thiols to cause inhibition of aldehyde dehydrogenase,<sup>6</sup> and it induces vasorelaxation through upregulation of calcitonin gene-related peptide.<sup>7</sup>

Several biochemical studies suggest that HNO can be formed by two-electron oxidation of hydroxylamine catalyzed by a heme enzyme.<sup>8</sup> Further, hydrogen sulfide (H<sub>2</sub>S) may be involved in its biosynthesis.<sup>9</sup> However, studies of the biological importance of HNO remain hampered by the lack of efficient HNO detection methods available in living cells.

Fluorescence detection is recognized to have both high sensitivity and high spatiotemporal resolution for visualizing biomolecules *in vitro* and *in vivo*. Several groups have developed fluorescent probes for HNO, but they are mostly based on the

reduction of Cu (II) to Cu (I),<sup>10,11</sup> or nitroxide to hydroxylamine, by HNO.<sup>12</sup> Therefore, those probes are vulnerable to biological reductants, such as glutathione (GSH) and ascorbate, which are abundant in living cells.

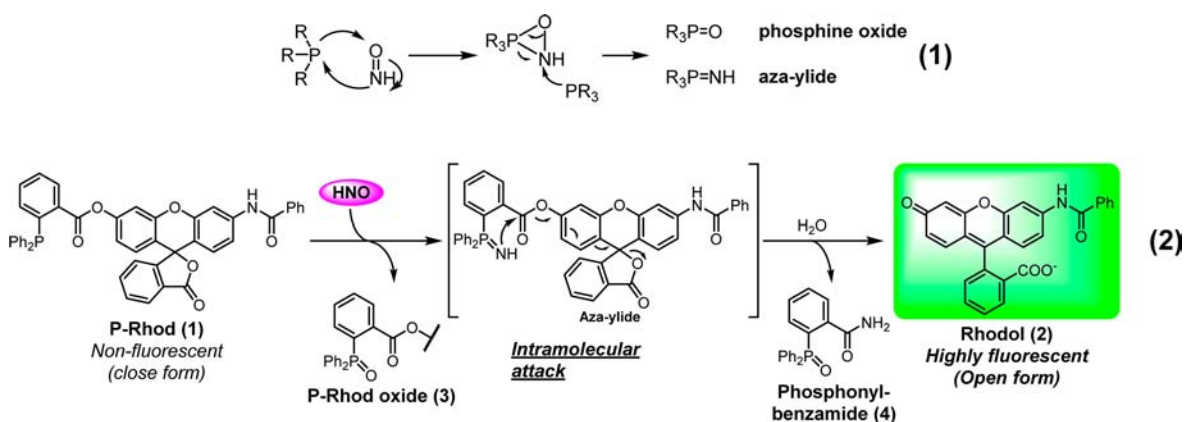
To overcome the issue of poor selectivity, we focused on the reaction between HNO and phosphine. It is known that HNO reacts with triarylphosphines to give the corresponding phosphine oxide and aza-ylide (Scheme 1, eq 1). In the presence of a properly situated electrophilic ester, intramolecular nucleophilic attack of the aza-ylide on the carbonyl carbon of the ester is expected to occur, leading to the formation of alcohol and amide.<sup>13,14</sup> Phosphines are abiotic and essentially unreactive toward biomolecules inside or on the surface of cells, so that aza-ylide formation by HNO is a bioorthogonal reaction.<sup>15</sup> Moreover, the reaction rate constant between HNO and phosphine derivative is sufficiently high (estimated as  $9 \times 10^5 \text{ M}^{-1}\text{s}^{-1}$ ) for the present purpose,<sup>14</sup> so we adopted triphenylphosphine as the HNO detecting moiety.

Rhodol, 2-(3-amino-6-oxoxanthene-9-yl)benzoic acid, has excellent photophysical properties, good solubility in various solvents, high fluorescence quantum yield, and good membrane permeability.<sup>16,17</sup> Further, it can adopt either of two tautomeric forms, the fluorescent xanthene form (open form) and the nonfluorescent lactone form (closed form). The closed form can be imposed on rhodol by acylation of both the amino

Received: May 13, 2013

Published: July 18, 2013

Scheme 1. Proposed Mechanisms of the Reaction of Phosphine with HNO (eq 1) and That of P-Rhod with HNO (eq 2)



group and phenolic hydroxyl group at the xantheno moiety, while the open form is in the preferred form of monoacylated rhodol (i.e., the amide form of rhodol) in aqueous solution.<sup>18</sup>

In the light of these facts, we designed a novel HNO fluorescent probe, named P-Rhod (1), consisting of rhodol acylated at its amino moiety, coupled to a triphenylphosphine moiety via an ester linker. Reaction between HNO and the phosphine moiety was expected to form an aza-ylide, and then intramolecular nucleophilic attack of the aza-ylide on carbonyl carbon would lead to release of rhodol 2 in the fluorescent open form, together with (diphenylphosphonyl)benzamide 4 (Scheme 1, eq 2). Therefore, P-Rhod should exhibit turn-on type fluorogenic behavior in response to HNO, and we anticipated that it would be able to detect HNO with high sensitivity and selectivity in living cells.

## EXPERIMENTAL SECTION

**General Methods.** Melting points were determined using a Yanaco micromelting point apparatus or a Büchi B-545 melting point apparatus and were left uncorrected. Proton and carbon nuclear magnetic resonance (<sup>1</sup>H and <sup>13</sup>C NMR, respectively) spectra were recorded on a JEOL JNM-LA500 or JEOL JNM-A500 spectrometer in the indicated solvent. Chemical shifts ( $\delta$ ) are reported in parts per million (ppm) relative to the internal standard, tetramethylsilane (TMS). Elemental analysis was performed with a Yanaco CHN CORDER NT-5 analyzer, and all values were within  $\pm 0.4\%$  of the calculated values. UV–vis light absorbance spectra were measured on an Agilent 8453 spectrometer. GC–MS analyses were performed on a Shimadzu GCMS-QP2010. FAB–MS were recorded on a JEOL JMS-SX102A mass spectrometer. Angeli's salt (AS) was obtained from Cayman Chemical, and ONOO<sup>−</sup> in NaOH solution, NOC 7, NOR 1, SNAP, and GSNO were obtained from Dojindo. All other reagents and solvents were purchased from Aldrich, Tokyo Kasei Kogyo, Wako Pure Chemical Industries, Nacalai Tesque, Kishida Kagaku, Junsei Kagaku, and Kanto Kagaku and used without further purification. Flash column chromatography was performed using silica gel 60 (particle size 0.046–0.063 mm) supplied by Taiko Shoji.

**Synthesis of 6.** To a suspension of fluorescein (50.0 g, 0.150 mol) and K<sub>2</sub>CO<sub>3</sub> (62.4 g, 0.451 mol) in 210 mL of anhydrous DMF was added chloromethyl methyl ether (48.5 g, 0.602 mol) at 0 °C under a nitrogen atmosphere. The reaction mixture was stirred at room temperature (rt) for 24 h, diluted with CHCl<sub>3</sub>, washed with 0.5 N HCl solution, water and brine, and then dried over Na<sub>2</sub>SO<sub>4</sub>. Filtration, concentration *in vacuo*, and purification by silica gel flash column chromatography (EtOAc:hexane = 1:1), followed by purification by silica gel flash column chromatography (CHCl<sub>3</sub>:MeOH = 20:1) gave 6.94 g (12%) of 6 as yellow crystals: <sup>1</sup>H NMR (CDCl<sub>3</sub>, 500 MHz,  $\delta$ ; ppm) 8.03 (1H, d, *J* = 7.6 Hz), 7.65 (2H, m), 7.17 (1H, d, *J* = 7.5 Hz),

6.97 (1H, d, *J* = 2.0 Hz), 6.71 (4H, m), 6.54 (1H, dd, *J* = 8.6 Hz, *J* = 2.5 Hz), 5.21 (2H, s), 3.49 (3H, s); MS(EI) *m/z*: 376 (M<sup>+</sup>).

**Synthesis of 7.** To a solution of 6 (6.00 g, 15.9 mmol) and pyridine (6.31 g, 79.7 mmol) in CH<sub>2</sub>Cl<sub>2</sub> was added dropwise trifluoromethanesulfonic anhydride (13.5 g, 47.8 mmol) at 0 °C under N<sub>2</sub> gas. The resulting solution was stirred at rt for 4 h, and then the reaction was quenched with water. CH<sub>2</sub>Cl<sub>2</sub> was added to the mixture, and the organic layer was separated and washed with 1 N HCl, followed by water and brine. The organic layer was dried over Na<sub>2</sub>SO<sub>4</sub> and concentrated. The residue was purified by silica gel column chromatography (EtOAc:hexane = 1:1) to give 5.48 g (69%) of 7 as white crystals: <sup>1</sup>H NMR (CDCl<sub>3</sub>, 500 MHz,  $\delta$ ; ppm) 8.05 (1H, d, *J* = 7.9 Hz), 7.67 (2H, m), 7.23 (1H, s), 7.18 (1H, d, *J* = 7.0 Hz), 6.95 (3H, m), 6.75 (2H, m), 5.21 (2H, s), 3.49 (3H, s); MS(EI) *m/z*: 508 (M<sup>+</sup>).

**Synthesis of 8.** An oven-dried flask was charged with Pd(OAc)<sub>2</sub> (0.484 g, 2.15 mmol), Xantphos (1.87 g, 3.23 mmol), and Cs<sub>2</sub>CO<sub>3</sub> (9.83 g, 30.2 mmol). A solution of 7 (5.48 g, 10.8 mmol) and benzamide (2.35 g, 19.3 mmol) in dioxane was added, and the resulting mixture was stirred under N<sub>2</sub> gas at rt for 30 min and then at 100 °C for 23 h. At that time the reaction mixture was allowed to cool to rt, diluted with CH<sub>2</sub>Cl<sub>2</sub>, and filtered through a pad of Celite. The filter cake was washed with CH<sub>2</sub>Cl<sub>2</sub>. The filtrate was concentrated, and the residue was purified by silica gel column chromatography (MeOH:CHCl<sub>3</sub> = 1:20) to give 3.96 g (77%) of 8 as pale-yellow crystals: <sup>1</sup>H NMR (CDCl<sub>3</sub>, 500 MHz,  $\delta$ ; ppm) 8.44 (1H, s), 7.97 (1H, d, *J* = 7.6 Hz), 7.86 (3H, m), 7.63 (2H, m), 7.50 (1H, dd, *J* = 7.3 Hz, *J* = 7.3 Hz), 7.42 (2H, dd, *J* = 7.9 Hz, *J* = 7.9 Hz), 7.14 (2H, m), 6.93 (1H, d, *J* = 2.0 Hz), 6.67 (3H, m), 5.18 (2H, s), 3.47 (3H, s); MS(FAB) *m/z*: 480 (M + 1)<sup>+</sup>.

**Synthesis of Rhodol 2.** To a solution of 8 (190 mg, 0.397 mmol) in CH<sub>2</sub>Cl<sub>2</sub> (6 mL) was added dropwise trifluoroacetic acid (6 mL) at 0 °C under N<sub>2</sub> gas. The resulting solution was stirred at rt for 16 h, then concentrated *in vacuo*, and azeotroped three times with toluene. Purification by silica gel flash column chromatography (CHCl<sub>3</sub>:MeOH = 20:1) gave 108 mg (63%) of crude product, which was recrystallized from CH<sub>2</sub>Cl<sub>2</sub>/hexane to afford 57 mg (33%) of 2 as an orange solid: mp 180.4–182.7 °C; <sup>1</sup>H NMR (CD<sub>3</sub>OD, 500 MHz,  $\delta$ ; ppm) 8.03 (1H, d, *J* = 7.7 Hz), 7.94 (3H, m), 7.79 (1H, dd, *J* = 7.4 Hz, *J* = 7.4 Hz), 7.72 (1H, dd, *J* = 7.5 Hz, *J* = 7.5 Hz), 7.59 (1H, dd, *J* = 7.4 Hz, *J* = 7.4 Hz), 7.52 (2H, dd, *J* = 7.8 Hz, *J* = 7.8 Hz), 7.35 (1H, dd, *J* = 8.6 Hz, *J* = 2.1 Hz), 7.24 (1H, d, *J* = 7.6 Hz), 6.74 (2H, m), 6.61 (1H, d, *J* = 8.7 Hz), 6.58 (1H, dd, *J* = 8.7 Hz, *J* = 2.4 Hz). <sup>13</sup>C NMR (CD<sub>3</sub>OD, 150 MHz,  $\delta$ ; ppm) 171.51, 169.07, 161.28, 154.53, 153.99, 153.14, 142.38, 136.71, 136.08, 133.16, 131.25, 130.19, 129.72, 129.55, 129.36, 128.74, 128.02, 125.90, 125.31, 117.50, 115.99, 113.75, 111.11, 109.53, 103.66. HRMS (FAB) calcd for C<sub>27</sub>H<sub>18</sub>NO<sub>5</sub>, 436.11849; found, 436.11956. HPLC *t<sub>R</sub>* = 8.10 min (purity 98.1%); anal. calcd for C<sub>27</sub>H<sub>17</sub>NO<sub>5</sub>·3/5 H<sub>2</sub>O: C, 72.67; H, 4.11; N, 3.14. Found: C, 72.60; H, 4.54; N, 3.26.

**Synthesis of P-Rhod (1).** **2** (1.11 g, 2.55 mmol), 2-(diphenylphosphino)benzoic acid (782 mg, 2.55 mmol), 4-(dimethylamino)pyridine (312 mg, 2.55 mmol), and 1-ethyl-3-(3-dimethylaminopropyl)carbodiimide hydrochloride (1.47 g, 7.66 mmol) were dissolved in THF. The reaction mixture was stirred for 22 h at rt under N<sub>2</sub> gas and then poured into 1 N HCl and extracted with CHCl<sub>3</sub>. The organic layer was separated, washed with sodium bicarbonate, water, and brine, and dried over Na<sub>2</sub>SO<sub>4</sub>. Filtration, concentration *in vacuo*, and purification by silica gel flash column chromatography (CHCl<sub>3</sub>:MeOH = 98:2 to CHCl<sub>3</sub>:MeOH = 95:5) gave 1.51 g (82%) of crude product, which was recrystallized from CH<sub>2</sub>Cl<sub>2</sub>/hexane to afford 817 mg (44%) of **6** as a pale-yellow solid. The product was purified by preparative HPLC: mp 154.5–156.4 °C; <sup>1</sup>H NMR (DMSO, 500 MHz, δ; ppm) 10.55 (1H, s), 8.26 (1H, m), 8.06 (2H, m), 7.97 (2H, m), 7.82 (1H, dd, *J* = 7.4 Hz, *J* = 7.4 Hz), 7.76 (1H, dd, *J* = 7.4 Hz, *J* = 7.4 Hz), 7.62 (3H, m), 7.55 (2H, dd, *J* = 7.7 Hz, *J* = 7.7 Hz), 7.49 (1H, dd, *J* = 8.6 Hz, *J* = 2.0 Hz), 7.39 (7H, m), 7.23 (4H, m), 7.14 (1H, d, *J* = 2.3 Hz), 6.92 (1H, m), 6.83 (3H, m). <sup>13</sup>C NMR (DMSO, 150 MHz, δ; ppm) 168.47, 165.92, 164.28 (d, <sup>4</sup>*J*<sub>P-C</sub> = 1.8 Hz), 152.35, 151.51, 150.93, 150.35, 141.45, 140.23 (d, <sup>2</sup>*J*<sub>P-C</sub> = 27.8 Hz), 136.94 (d, <sup>1</sup>*J*<sub>P-C</sub> = 11.0 Hz), 135.83, 134.37, 133.71, 133.44 (d, <sup>2</sup>*J*<sub>P-C</sub> = 20.8 Hz), 133.03, 132.53 (d, <sup>2</sup>*J*<sub>P-C</sub> = 19.2 Hz), 131.82, 131.15, 130.33, 129.03, 128.95, 128.84, 128.70 (d, <sup>3</sup>*J*<sub>P-C</sub> = 7.2 Hz), 128.57, 128.36, 128.22, 127.67, 125.38, 124.84, 123.96, 118.02, 116.55 (d, <sup>3</sup>*J*<sub>P-C</sub> = 5.3 Hz), 113.13, 110.36, 107.14, 81.242. <sup>31</sup>P NMR (DMSO, 243 MHz, δ; ppm) –5.041; MS (FAB) *m/z*: 724 (M + 1)<sup>+</sup>. Anal. calcd for C<sub>46</sub>H<sub>30</sub>N<sub>6</sub>O<sub>6</sub> P<sub>3</sub>/5 H<sub>2</sub>O: C, 75.22; H, 4.28; N, 1.91. Found: C, 74.83; H, 4.38; N, 2.00.

**HPLC Analysis.** HPLC analysis was performed on an Inertsil ODS-3 (150 mm × Φ4.6 mm) column (Shenshu Pak C18) using a Shimadzu HPLC system. Detection wavelength was 254 nm. Injection volume was 20 μL. Flow rate was 1.0 mL/min.

**Preparative HPLC.** Preparative HPLC was performed on an Inertsil ODS-3 (250 mm × Φ20 mm) column (Shenshu Pak C18) using an HPLC system composed of a pump and a detector (Shimadzu). Injection volume was 100–500 μL.

**HPLC Analysis for Detection of Rhodol 2.** Sample solutions (total volume 1.0 mL) of 100 μM P-Rhod in 100 mM potassium phosphate buffer containing 1% DMF were incubated for 30 min at 37 °C after addition of 100 or 2000 μM AS. An aliquot of each solution (20 μL) was loaded onto a Shenshu Pak C18 column fitted on a Shimadzu HPLC system, and the eluates were monitored with a photodiode array detector and fluorescence detector. Milli-Q water containing 0.1% TFA (A) and MeCN containing 0.1% TFA (B) were used as developing solvents. Gradient conditions were as follows: A 15% and B 85% for 20 min, then to A 60% and B 40% for 33 min and continued for 3 min.

**Fluorescence Measurement of P-Rhod *in Vitro*.** Fluorescence spectra were measured with a Shimadzu RF5300-PC. The slit width was set to 5.0 nm for excitation and emission. P-Rhod was freshly dissolved in DMF to obtain 10 mM solution, and the solutions were diluted to 10 μM with 100 mM PBS buffer (pH 7.4). An aliquot of a freshly prepared stock solution of reagents was added to a buffered solution of the test compounds to give final concentrations of 10 μM test compound and the indicated concentrations of RNS, ROS, or biomolecules. The reaction mixture (total volume = 1 mL) was incubated for 30 min at 37 °C, then the fluorescence spectrum (490–650 nm) was measured with excitation at 491 nm.

**Detection of N<sub>2</sub>O by Gas Chromatography.** A solution of hydroxylamine hydrochloride with or without HRP in Tris buffer (500 mM, 0.2 mM EDTA, pH 7.4, 0.5 mL containing 0.1% DMSO as a cosolvent) was placed in a 5 mL vial sealed with a rubber septum and flushed with nitrogen gas. To initiate the reaction, hydrogen peroxide was added to the solution, and the vials were then incubated for 2 h at 37 °C. An aliquot of the reaction headspace gas (50 μL) was injected into a Shimadzu GC-2010 gas chromatograph equipped with a mass spectrometer (QP2010) and a Rt-QPLOT column (0.32 mm × 15 m) expanded with a 15 m inactivated fused silica tube (total 30 m). The GC injector was operated with a split ratio of 0.1 at 200 °C. The carrier gas (He) was set at a flow rate of 2.2 mL/min. The GC oven was held at 35 °C. The MS interface was set to 280 °C.

**Detection of Enzymatic HNO Generation via HRP-Mediated Oxidation of Hydroxylamine.** A deoxygenated solution of P-Rhod (0.5 μL, 10 μM), hydroxylamine hydrochloride (10 μL, 10 mM), and horseradish peroxidase (HRP) type I (10 μL, 20 μM) in Tris buffer (1.0 M, 0.4 mM EDTA, pH 7.4, 0.25 mL) was prepared at ambient temperature in a septum-sealed vial. Hydrogen peroxide (10 μL, 10 mM) was added to initiate the reaction. After 2 h at 37 °C, the resulting solution (0.5 mL) was examined with a fluorophotometer to evaluate fluorescence enhancement. Control experiments involving exclusion of any one of the reaction components did not exhibit fluorescence enhancement.

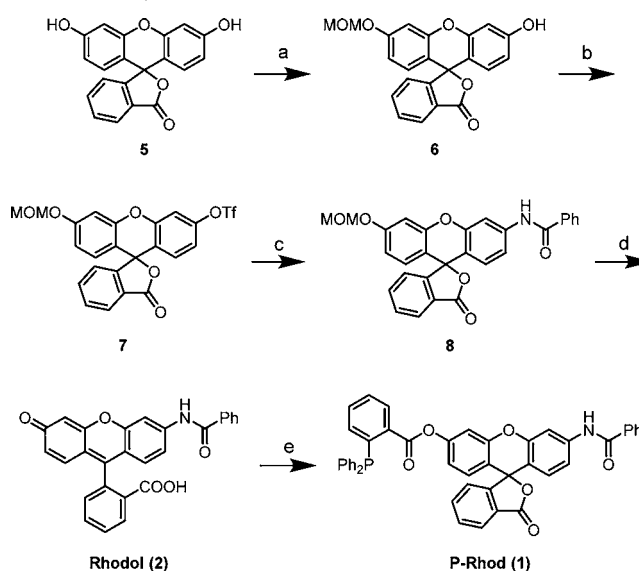
**Cell Culture.** A549 cells were purchased from the RIKEN Cell Bank and cultured in DMEM containing 10% FBS and penicillin/streptomycin (100 U/mL) in a humidified incubator at 37 °C. When the cells had reached confluence, they were detached in trypsin solution, washed in DMEM, centrifuged at 125 *g* for 2 min, and then resuspended and subcultured according to standard protocols.

**Detection of HNO in A549 Cells.** A549 cells were plated onto 3.5 cm glass-bottomed culture dishes at 1.0 × 10<sup>5</sup> cells/dish with 2.0 mL of DMEM containing penicillin and streptomycin, supplemented with FBS, according to ATCC's instructions, and incubated at 37 °C in a humidified 5% (v/v) CO<sub>2</sub> incubator for 1 day. The culture medium was then removed, and the cells were washed once with 1 mL of Dulbecco's PBS (D-PBS). They were placed in 1 mL of D-PBS and treated with 1 μL of P-Rhod (1 δM) for 3 h, then washed twice with 1 mL of D-PBS and placed in 1 mL of D-PBS. The cells were then treated with 2 μL of AS in 10 mM NaOH solution (200 μM), 2 μL of 10 mM NaOH solution, 1 μL of NOC 7 in 10 mM NaOH solution (100 μM), 10 μL of GSNO in water (100 μM), or 1 μL of NaClO in water (1 μM), and subjected to confocal microscopy. Imaging was performed with a 63× oil-immersion objective lens on a Zeiss LSM 510 laser scanning microscope.

## RESULTS AND DISCUSSION

P-Rhod was synthesized as shown in Scheme 2, according to Dan's synthetic strategy.<sup>18</sup> Briefly, the synthesis of P-Rhod was

### Scheme 2. Synthesis of P-Rhod<sup>α</sup>



<sup>α</sup>Reagents and conditions: (a) CH<sub>3</sub>OCH<sub>2</sub>Cl, K<sub>2</sub>CO<sub>3</sub>, DMF; (b) (CF<sub>3</sub>SO<sub>2</sub>)<sub>2</sub>O, pyridine, CH<sub>2</sub>Cl<sub>2</sub>; (c) Pd(OAc)<sub>2</sub>, 4,5'-bis(diphenylphosphino)-9,9'-dimethylxanthene, Cs<sub>2</sub>CO<sub>3</sub>, benzamide, dioxane; (d) CF<sub>3</sub>COOH, CH<sub>2</sub>Cl<sub>2</sub>; (e) 2-(diphenylphosphino)benzoic acid, EDCl, DMAP, THF. DMF = *N,N*-dimethylformamide, EDCl = 1-ethyl-3-(3-dimethylaminopropyl)carbodiimide hydrochloride, DMAP = *N,N*-dimethyl-4-aminopyridine, THF = tetrahydrofuran.

started from commercially available fluorescein 5, which was first monoprotected with a methoxymethyl (MOM) group. The protected fluorescein 6 was triflated to provide doubly protected fluorescein 7, which was coupled with benzamide by using Pd catalyst to obtain amide derivative 8. The MOM group of 8 was easily removed under acidic conditions to afford a rhodol fluorophore 2, which was subjected to esterification to yield P-Rhod (1). The structure and purity of P-Rhod were confirmed by  $^1\text{H}$ ,  $^{13}\text{C}$ , and  $^{31}\text{P}$  NMR spectroscopy, mass spectrometry, and elemental analysis.

First, the photophysical properties of rhodol 2 were assessed in a buffer solution (100 mM potassium phosphate buffer, pH 7.4, 0.1% DMF). The compound was found to have typical optical properties of a rhodol chromophore, with an absorption band in the blue range centered at 491 nm ( $\epsilon = 2.95 \times 10^4 \text{ M}^{-1} \text{ cm}^{-1}$ ). The emission profile was also typical of rhodol, showing green fluorescence with a maximum at 526 nm. The fluorescence quantum yield of 2 has been reported.<sup>18</sup> When rhodol 2 was esterified to afford P-Rhod, the fluorescence intensity decreased by ca. 774-fold (Figure 1). This remarkable

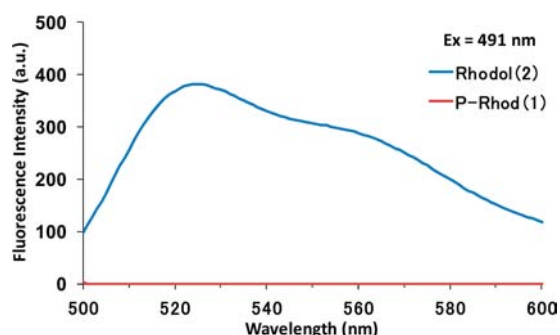


**Figure 1.** Fluorescence spectra of 10  $\mu\text{M}$  rhodol 2 (top line) and P-Rhod (bottom line).

change of the fluorescence intensity can be attributed to the open–closed form conversion of rhodol, due to acylation of the phenolic hydroxyl group of 2.

P-Rhod (10  $\mu\text{M}$ ) was readily soluble in water in the presence of 0.1% DMF, suggesting that it might be suitable for use in living cells. The absorption band of P-Rhod at 491 nm was small ( $\epsilon = 9.58 \text{ M}^{-1} \text{ cm}^{-1}$ ), and the fluorescence was too weak to be detected. Thus, P-Rhod was essentially nonfluorescent, due to its unconjugated and nonfluorescent closed form resulting from acylation of the amino and hydroxyl groups at the xanthene moiety. It is considered that an ester group is generally labile under acidic or basic conditions. However, the fluorescence intensity of P-Rhod, despite its ester group, was independent of pH over the range of pH 5.0–10.0 (see Figure S1). This would be highly advantageous for biological applications, considering the different pH conditions in various cellular compartments.

We next examined whether P-Rhod could detect HNO under physiological conditions. A buffer solution containing 10  $\mu\text{M}$  P-Rhod was incubated at 37  $^\circ\text{C}$  for 30 min in the presence of 200  $\mu\text{M}$  AS, which spontaneously generates an equimolar ratio of HNO and  $\text{NO}_2^-$  under physiological conditions.<sup>19</sup> After incubation, the fluorescence intensity at 526 nm was significantly increased (Figure 2) and reached maximum in ca. 20 min (Figure S2). We assessed the selectivity of P-Rhod for HNO over other reactive species present in the biological milieu. RNS and reactive oxygen species (ROS) donors and oxidants ( $\text{ONOO}^-$ ,  $\text{NO}_2^-$ ,  $\text{NO}_3^-$ ,  $\text{H}_2\text{O}_2$ ,  $\text{ClO}^-$ , and  $\text{FeCl}_3$ ) did

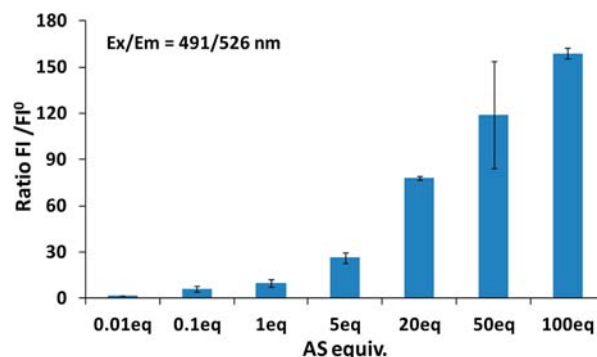


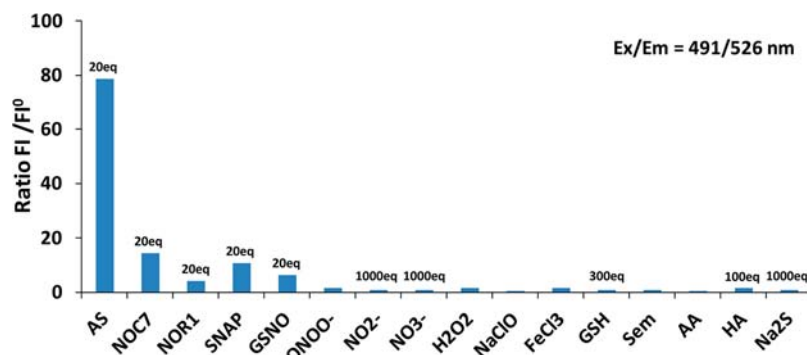
**Figure 2.** Fluorescence responses of 10  $\mu\text{M}$  P-Rhod to 0.1, 1, 10, 50, 200, 500, or 1000  $\mu\text{M}$  AS in 100 mM potassium phosphate buffer (pH 7.4) containing 1% DMF after 30 min incubation at 37  $^\circ\text{C}$ . Means  $\pm$  SD.

not induce significant fluorescence enhancement of P-Rhod (Figure 3). It is particularly noteworthy that the fluorescence intensity of P-Rhod was hardly affected by biological reductants, including GSH, selenomethionine (Sem), ascorbic acid (AA), and hydroxylamine (HA) as well as sodium sulfide ( $\text{Na}_2\text{S}$ ), which works as a source of  $\text{H}_2\text{S}$  under physiological conditions. In this regard, P-Rhod is greatly superior to the previously reported  $\text{Cu}^{\text{II}}$ -based probes, which show substantial fluorescence in the presence of large amounts of various biological reductants.<sup>10a</sup> When 10  $\mu\text{M}$  P-Rhod in a buffered aqueous solution was treated with various amounts of AS, the fluorescence intensity increased concentration dependently (Figure 2), and 100 nM AS induced a 1.49-fold increase in fluorescence intensity compared to the blank. Additionally, even when a solution of AS and HNO was incubated in the presence of various ROS or RNS, we successfully detected sufficient fluorescence. (Figure S3). Such high sensitivity for HNO is advantageous for the detection in physiological condition.

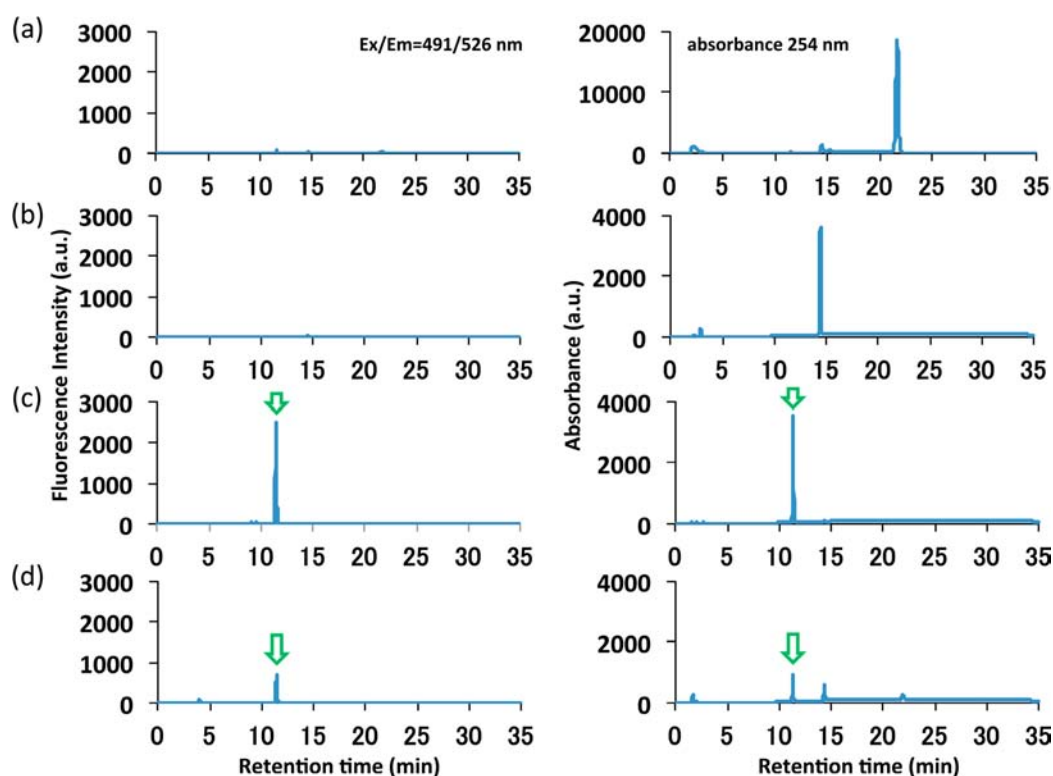
While P-Rhod did not react with various RNS and ROS, as shown in Figure 3, SNAP and GSNO were found to increase the fluorescence slightly (Figure S4). Tris(4,6-dimethyl-3-sulfonatophenyl)phosphine trisodium salt (TXPTS) has been reported to react with RSNO, generating phosphine oxide, aza-ylide, and S-phosphino adduct.<sup>20</sup> Thus, there might be a direct reaction between P-Rhod and these NO donors or nitroxyl anion ( $\text{NO}^-$ ) generated by one-electron reduction of NO radical by phosphine. However, the fluorescence increase of P-Rhod with SNAP and GSNO was small, suggesting that the practical selectivity of P-Rhod for HNO is sufficient. We speculate that steric hindrance of the xanthene moiety of P-Rhod reduced the reactivity with RSNO groups. Also, RSNO groups require 3 equiv of phosphine to yield aza-ylide, the key intermediate to form rhodol 2, while HNO requires only 2 equiv.

When the reaction of P-Rhod and AS was performed in the presence of GSH, a scavenger of HNO,<sup>21</sup> the fluorescence intensity decreased with increasing GSH concentration (Figure S5). Further, 1000  $\mu\text{M}$   $\text{NaNO}_2$ , formed after HNO release from AS, did not affect the fluorescence of 10  $\mu\text{M}$  P-Rhod. Moreover, the fluorescent intensity of Rhodol 2 was not decreased after incubation with GSH or the reaction mixture of AS and GSH. These results strongly suggest that the turn-on response induced by AS is due to HNO production and not due to a byproduct.

Next, to confirm that P-Rhod is converted to the expected product, rhodol 2, after incubation (30 min at 37  $^\circ\text{C}$ ) of a solution containing AS and P-Rhod, the sample solution was analyzed by HPLC (Figure 4). The proposed mechanism of the



**Figure 3.** Fluorescence responses of 10  $\mu\text{M}$  P-Rhod in 100 mM potassium phosphate buffer (pH 7.4) containing 0.1% DMF at 37  $^{\circ}\text{C}$  for 30 min after addition of the following substances: AS, NOC 7, NOR 1, SNAP, GSNO, ONOO $^{-}$ , NO $_2^{-}$ , NO $_3^{-}$ , H $_2$ O $_2$ , NaClO, FeCl $_3$ , GSH, selenomethionine (Sem), ascorbic acid (AA), hydroxylamine (HA) and sodium sulfide (Na $_2$ S). Unless otherwise indicated in the figure, 400 equiv of each analyte were added. Bars represent the ratio of the observed intensity (FI) to the control (FI $^0$ ) emission at 526 nm.

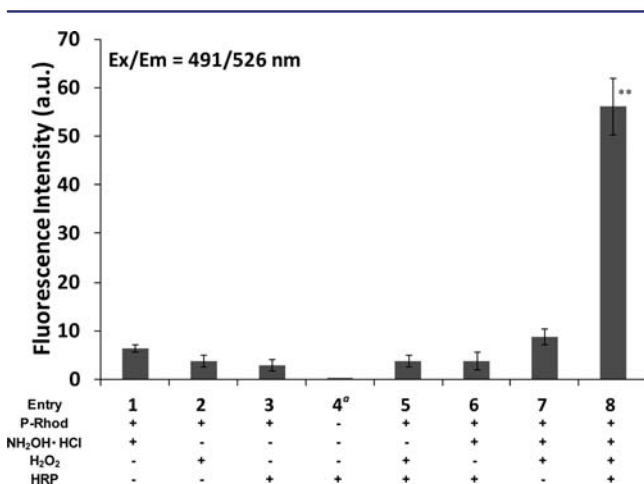
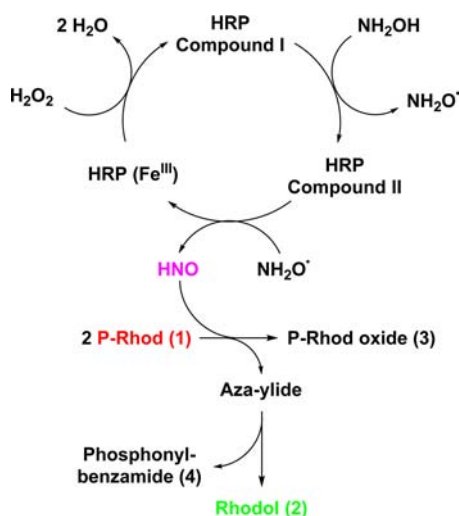


**Figure 4.** Reversed-phase HPLC chromatograms with fluorescence (left) and absorption (right) detection. The arrow indicates rhodol 2. Excitation: 491 nm, emission: 526 nm. (a) An authentic solution of 1000  $\mu\text{M}$  P-Rhod. (b) An authentic solution of 100  $\mu\text{M}$  P-Rhod oxide 3. (c) An authentic solution of 100  $\mu\text{M}$  rhodol 2. (d) A sample solution of 100  $\mu\text{M}$  P-Rhod with 2000  $\mu\text{M}$  AS in 100 mM potassium phosphate buffer (pH 7.4, 0.1% DMF) after incubation for 30 min at 37  $^{\circ}\text{C}$ .

reaction of P-Rhod with HNO is shown in eq 2 of Scheme 1. P-Rhod reacts with HNO to give P-Rhod oxide 3, phosphonylbenzamide 4, and rhodol 2. As shown in Figure 4d, rhodol 2 and P-Rhod oxide 3 were detected concomitantly with the decrease of P-Rhod in the incubated solution, although phosphonylbenzamide 4 could not be detected, probably due to its extremely small extinction coefficient. Although P-Rhod was slightly hydrolyzed in the solution without AS, as shown by weak fluorescence of rhodol 2 in the control solution (Figure 4a), the fluorescence intensity was negligible as compared with that of a solution of P-Rhod with AS. These results support the proposed mechanism of reaction of P-Rhod with HNO.

We next investigated whether P-Rhod could detect HNO generated from an enzymatic system. A heme protein, HRP,

was employed for the detection of HNO generated enzymatically *in vitro*. One of proposed biosynthetic pathways of HNO is two-electron oxidation of NH $_2$ OH catalyzed by HRP (Scheme 3).<sup>8</sup> Anaerobic incubation of NH $_2$ OH (10 mM) and H $_2$ O $_2$  (10 mM) in the presence of HRP (20  $\mu\text{M}$ ) for 2 h at 37  $^{\circ}\text{C}$  afforded N $_2$ O, a dimerization product of HNO, as determined by GC-MS using N $_2$ O derived from AS as a positive control. No N $_2$ O was produced in the incubation solution in the absence of HRP (Figures S6 and S7).<sup>14</sup> P-Rhod was added to this enzymatic system before H $_2$ O $_2$  addition. After the addition of H $_2$ O $_2$ , the fluorescence intensity increased (Figure 5). No marked fluorescence increase was observed in the absence of NH $_2$ OH, H $_2$ O $_2$ , or HRP in the incubation mixture, indicating that the fluorescence increase depended on the HRP system.

Scheme 3. Mechanism of HRP-mediated HNO formation from  $\text{NH}_2\text{OH}$ 

**Figure 5.** Fluorescence enhancement of P-Rhod ( $10 \mu\text{M}$ ) in the presence or absence of hydroxylamine hydrochloride ( $10 \text{ mM}$ ), HRP type I ( $20 \mu\text{M}$ ), or hydrogen peroxide ( $10 \text{ mM}$ ) in Tris buffer ( $500 \text{ mM}$ ,  $0.2 \text{ mM}$  EDTA,  $\text{pH } 7.4$ ) for 2 h at  $37^\circ\text{C}$ . (a)  $0.1\%$  DMSO was added instead of P-Rhod in the solution of entry 4. Means  $\pm$  SD  $^{**}p < 0.01$  compared with entries 5–7 by ANOVA and Bonferroni-type multiple  $t$ -test (parametric,  $n = 3$ ).

These results demonstrate that P-Rhod can efficiently detect enzymatically generated HNO.

Next, we applied P-Rhod for the detection of HNO in living cells. Human alveolar basal epithelial A549 adenocarcinoma cells were incubated with  $1 \mu\text{M}$  P-Rhod for 3 h at  $37^\circ\text{C}$ . Under this condition, the cells showed little intracellular fluorescence (Figure 6a), indicating that P-Rhod was not susceptible to intracellular hydrolysis. Addition of  $200 \mu\text{M}$  AS to the cells increased the intracellular fluorescence 11-fold during a further 20 min incubation (Figure 6b–d), as quantified by using Image J software. The fluorescence intensity in the cells appeared to be predominantly localized in cytoplasm. Although there is plenty of GSH, a scavenger of HNO, in a living cell, we successfully detected HNO from AS with P-Rhod. It might be because the excellent sensitivity of P-Rhod enabled to visualize HNO, while the reaction of HNO with P-Rhod could be minor compared to that with GSH. In the control experiment (vehicle treatment), no change in fluorescence intensity was seen (Figure S8). This result suggested that the ester moiety of P-Rhod was not so sensitive for intracellular esterase, probably due to the bulkiness around the ester bond in this molecule. Treatment of P-Rhod-preloaded A549 cells with NOC 7 ( $100 \mu\text{M}$ ) or GSNO ( $100 \mu\text{M}$ ) did not affect the observed fluorescence (Figures S9 and S10). Moreover, no fluorescence increase was induced by addition of equimolar exogenous NaClO, an oxidant, to the cells containing P-Rhod (Figure S11). Taken together, these results confirm that P-Rhod is available for detection of HNO in living cells.

## CONCLUSION

We designed a fluorogenic HNO probe, P-Rhod, by utilizing the combination of aza-ylide formation via reaction of triarylphosphine with HNO and the open–closed tautomerism of rhodol fluorophore. The fluorescence increase was AS concentration dependent, and the probe was highly sensitive and selective for HNO over other biologically relevant RNS and ROS. A key advantage of P-Rhod is that it is unaffected by various biological reductants, in contrast to previously reported probes. Formation of the expected decomposition product of P-Rhod with AS was confirmed by HPLC analysis. P-Rhod could also detect HNO generated in the  $\text{NH}_2\text{OH}$ -HRP enzymatic system, which is believed to operate for HNO generation *in vivo*.

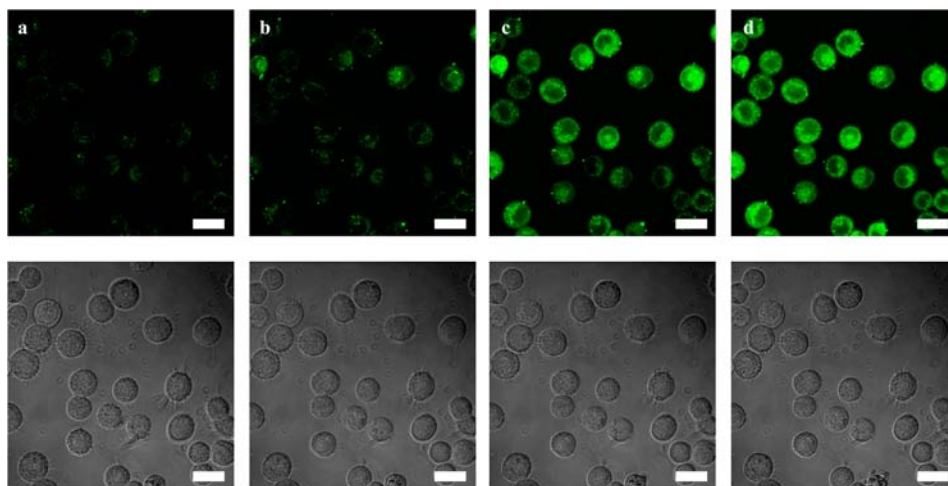


**Figure 6.** HNO-induced fluorescence images of A549 cells stained with  $1 \mu\text{M}$  P-Rhod before (a) and at 10 min (b), 15 min (c) and 20 min (d) after treatment with  $2 \mu\text{L}$  of AS in  $10 \text{ mM}$  NaOH solution ( $200 \mu\text{M}$ ): (top) FITC channels and (bottom) DIC images. Scale bars represent  $20 \mu\text{m}$ .

P-Rhod successfully imaged HNO intracellularly released from AS, with excellent selectivity over other ROS and RNS. Thus, P-Rhod is the first metal-free fluorescent molecular probe available for detection of HNO in living cells, and it is expected to be a useful chemical tool for studies of the biological roles of HNO.

## ■ ASSOCIATED CONTENT

### ■ Supporting Information

Supporting figures, syntheses of **3** and **4**,  $^1\text{H}$  NMR spectra for P-Rhod, **3** and **4**. This material is available free of charge via the Internet at <http://pubs.acs.org>.

## ■ AUTHOR INFORMATION

### Corresponding Author

deco@phar.nagoya-cu.ac.jp

### Present Address

<sup>†</sup>Graduate School of Medical Sciences, Kyoto Prefectural University of Medicine, 13 Taishogun Nishitakatsukasa-cho, Kita-ku, Kyoto 403–8334, Japan

### Notes

The authors declare no competing financial interest.

## ■ ACKNOWLEDGMENTS

This work was supported by JST PRESTO program (H.N.), Grants-in-Aid for Scientific Research on Innovative Areas (Research in a Proposed Research Area) (no. 21117514 to H.N.), and Grants-in-Aid for Scientific Research (no. 22590103 to H.N.) from Ministry of Education, Culture, Sports Science and Technology Japan.

## ■ REFERENCES

- (1) Fukuto, J. M.; Bartberger, M. D.; Dutton, A. S.; Paolucci, N.; Wink, D. A.; Houk, K. N. *Chem. Res. Toxicol.* **2005**, *18*, 790–801.
- (2) Moncada, S.; Palmer, R. M. J.; Higgs, E. A. *Pharmacol. Rev.* **1991**, *43*, 109–142.
- (3) Ieda, N.; Nakagawa, H.; Peng, T.; Yang, D.; Suzuki, T.; Miyata, N. *J. Am. Chem. Soc.* **2012**, *134*, 2563–2568.
- (4) Dedon, P. C.; Tannenbaum, S. R. *Arch. Biochem. Biophys.* **2004**, *423*, 12–22.
- (5) (a) Fukuto, J. M.; Cisneros, C. J.; Kinkade, R. L. *J. Inorg. Biochem.* **2013**, *118*, 201–208. (b) Paolucci, N.; Wink, D. A. *Am. J. Physiol.: Heart Circ. Physiol.* **2009**, *296*, H1217–H1220. (c) Miranda, K. M.; Paolucci, N.; Katori, T.; Thomas, D. D.; Ford, E.; Bartberger, M. D.; Espey, M. G.; Kass, D. A.; Feelisch, M.; Fukuto, J. M.; Wink, D. A. *Proc. Natl. Acad. Sci. U.S.A.* **2003**, *100*, 9196–9201.
- (6) DeMaster, E. G.; Redfern, B.; Nagasawa, H. T. *Biochem. Pharmacol.* **1998**, *55*, 2007–2015.
- (7) (a) Miranda, K. M.; Katori, T.; Torres de Holding, C. L.; Thomas, L.; Rindnour, L. A.; McLendon, W. J.; Cologne, S. M.; Dutton, A. S.; Champion, H. C.; Mancardi, D.; Tocchetti, C. G.; Saavedra, J. E.; Keefer, L. K.; Houk, K. N.; Fukuto, J. M.; Kass, D. A.; Paolucci, N.; Wink, D. A. *J. Med. Chem.* **2005**, *48*, 8220–8228. (b) Paolucci, N.; Saavedra, J. E.; Wink, D. A. *J. Med. Chem.* **2005**, *48*, 8220–8228.
- (8) F., W.; Miranda, K. M.; Martignani, C.; Isoda, T.; Hare, J. M.; Espey, M. G.; Fukuto, J. M.; Feelisch, M.; Wink, D. A.; Kass, D. A. *Proc. Natl. Acad. Sci. U.S.A.* **2001**, *98*, 10463–10468.
- (9) Donzelli, S.; Espey, M. G.; Flores-Santana, W.; Switzer, C. H.; Yeh, G. C.; Huang, J.; Stuehr, D. J.; King, S. B.; Miranda, K. M.; Wink, D. A. *Free Radical Biol. Med.* **2008**, *45*, 578–584.
- (10) (a) Rosenthal, J.; Lippard, S. J. *J. Am. Chem. Soc.* **2010**, *132*, 5536–5537. (b) Royzen, M.; Wilson, J. J.; Lippard, S. J. *J. Inorg. Biochem.* **2013**, *118*, 162–170. (c) Zhou, Y.; Liu, K.; Li, J. Y.; Fang, Y.; Zhao, T. C.; Yao, C. *Org. Lett.* **2011**, *13*, 1290–1293.
- (11) Kitamura, N.; Hiraoka, T.; Tanaka, K.; Chujo, Y. *Bioorg. Med. Chem.* **2012**, *20*, 4668–4674.

- (12) Cline, M. R.; Toscano, J. P. *J. Phys. Org. Chem.* **2011**, *24*, 993–998.
- (13) Reisz, J. A.; Klorig, E. B.; Wright, M. W.; King, S. B. *Org. Lett.* **2009**, *11*, 2719–2721.
- (14) Reisz, J. A.; Zink, C. N.; King, S. B. *J. Am. Chem. Soc.* **2011**, *133*, 11675–11685.
- (15) Saxon, E.; Bertozzi, C. R. *Science* **2000**, *287*, 2007–2010.
- (16) Whitaker, J. E.; Haugland, R. P.; Ryan, D.; Hewitt, P. C.; Haugland, R. P.; Prendergast, F. G. *Anal. Biochem.* **1992**, *207*, 267–279.
- (17) (a) Peng, T.; Yang, D. *Org. Lett.* **2010**, *12*, 4932–4935. (b) Kamiya, M.; Asanuma, D.; Kuranaga, E.; Takeishi, A.; Sakabe, M.; Miura, M.; Nagano, T.; Urano, Y. *J. Am. Chem. Soc.* **2011**, *133*, 12960–12963.
- (18) Peng, T.; Yang, D. *Org. Lett.* **2010**, *12*, 496–499.
- (19) Liochev, S. I.; Fridovich, I. *Free Radical Biol. Med.* **2003**, *34*, 1399–1404.
- (20) (a) Bechtold, E.; Reisz, J. A.; Klomsiri, C.; Tsang, A. W.; Wright, M. W.; Poole, L. B.; Furdul, C. M.; King, S. B. *ACS Chem. Biol.* **2010**, *5*, 405–414. (b) Zhang, J.; Wang, H.; Xian, M. *J. Am. Chem. Soc.* **2009**, *131*, 3854–3855. (c) Zhang, J. M.; Wang, H.; Xian, M. *Org. Lett.* **2009**, *11*, 477–480.
- (21) Irvine, J. C.; Ritchie, R. H.; Favaloro, J. L.; Andrews, K. L.; Widdop, R. E.; Kemp-Harper, B. K. *Trends Pharmacol. Sci.* **2008**, *29*, 601–608.